International Journal of Ambient Energy
Publication details, including instructions for authors and subscription information:
http://www.tandfonline.com/loi/taen20

Experimental study and simulation of a solar dryer for spearmint leaves (Mentha spicata)

Benaouda Nour-Eddine [a] , Zeghmati Belkacem [b] & Khellaf Abdellah [a]

[a] Centre for Renewable Energy Development, Solar Thermal and Geothermal Division , B.P. 62 Route de l'observatoire, Bouzaréah, Algier , Algeria

[b] LA.M.P. S., Univ. Perpignan Via Domitia , 52, avenue Paul Alduy 66860 Perpignan, France

Accepted author version posted online: 02 Jul 2013.

To cite this article: International Journal of Ambient Energy (2013): Experimental study and simulation of a solar dryer for spearmint leaves (Mentha spicata), International Journal of Ambient Energy, DOI: 10.1080/01430750.2013.820149

To link to this article: http://dx.doi.org/10.1080/01430750.2013.820149

Experimental study and simulation of a solar dryer for spearmint leaves (Mentha spicata)

Benaouda Nour-Eddine [a], Zeghmati Belkacem [b,1], Khellaf Abdellah [a]

[a] *Centre for Renewable Energy Development, Solar Thermal and Geothermal Division B.P. 62 Route de l'observatoire, Bouzaréah, Algier, Algeria.*
n_benaouda@cder.dz
[b] *LA.M.P. S., Univ. Perpignan Via Domitia, 52, avenue Paul Alduy 66860 Perpignan, France*
zeghmati@univ-perp.fr

Abstract

An indirect forced convection solar dryer consisting of an air flat plate collector and a drying cabined was designed and fabricated to investigate its performance under the climate of Algiers. Drying experiments have been performed for spearmint leaves at different air flow rate in order to determine the drying velocity, the characteristic drying curve, the effective diffusion coefficient and the activation energy. A mathematical model based on thermal and mass balances over the component of the solar collector and the cabinet dryer was developed. Simulations are carried out for meteorological data of Algiers (Algeria). We analyze the effect of air mass flow rate, air temperature, products mass, collector area, air recycling rate on the drying time, the solar fraction and the efficiency of the dryer.

Keywords: Solar drying, Curve drying characteristics, Drying efficiency, Simulation, Solar fraction

Nomenclature

Ac: collector area
Cp: specific heat ($J.kg^{-1}.K^{-1}$)
CDC: characteristic drying curve
D_{eff}: Diffusion coefficient ($m^2.s^{-1}$)
e: thickness (m)
f: solar fraction (%)
f*: dimensionless drying rate
h: heat transfer coefficient ($W.m^{-2}K^{-1}$)
L_V: latent heat of evaporation ($J.kg^{-1}$)
L: length (m)
m: mass (kg)
$\dot{m}$: air mass flow rate ($kg\ s^{-1}$)
$P_{0:}$ porosity
P: solar flux density ($W.m^{-2}$)
Q: quantity of heat (J)
RH: air relative humidity (%)
T: temperature (K)
t: time (s)
T_R: air recycling rate (%)
v: velocity ($m.s^{-1}$)

(1) Corresponding author : Tel :00(33)468661771 Fax : 00(33)468662075
Email address :zeghmati@univ-perp.fr

w: absolute humidity (kg (water) .kg^{-1} (dry air))
W : width (m)
X: moisture content (kg (water) .kg^{-1} (d.m))

Subscripts
0: initial
*: normalize, precedent tray
a: ambient
aux : auxillary
c: convection
co: solar collector
cri : critical moisture content
d: conduction
dry: dry, dryer, drying
e: external
eq : equilibrium moisture content
f: air
final: final
g: cover
i: internal
in: inlet
ins: insulation
j, k: index
M: mixing
out: outlet
p : absorber plate
pr: product
r : radiation
ray : tray
s: sky
t: top
U : useful
vp: vapor
w: wall
dif: diffuse
dir: direct
G: global
Ls, Cs: sunset, sunrise

Greeks
α: absorption coefficient
$\eta_{D,C}$:drying or solar collector efficiency (%)
$\sigma_{s:}$ source term
τ: transmittance
ΔS: elemental area (m^2)
Δt: time

1. Introduction

It is well know that the traditional open sun drying method practiced widely by rural farmers has inherent limitations as a high crop losses due to inadequate drying, insects, birds, rain and others weathering effects. Therefore, the quality of the dried product is often degraded seriously, sometimes not edible. A vast amount of works relates to solar dryers for various agricultural products have been conducted by many authors. In broad terms, they can be classified in two major groups: experimental and theoretical studies. The purpose of the mathematical modeling of the drying process is to allow design engineers to choose the most suitable operating conditions and size the drying cabinet and drying equipment accordingly to meet desired operating conditions. Models that describe the drying phenomena can be developed on mechanistic or empirical basis. However, the drying process is the subject of various phenomena (shrinkage, drying rate,...) which are very difficult to modeling. Consequently, experimental works are used in order to determine by fitting to mathematical models the drying rate, the diffusion coefficient. In this section, we attempt to report some papers about mathematical modeling and experimental studies: Concerning the theoretical works**,** Pratato et al. [1] developed a simplified design tool for sizing solar assisted fixed bed batch dryer for natural granulated natural rubber. It is assumed that drying conditions are constant during the drying. The tool is based on a relation describing the heat savings fraction for sizing solar assisted fixed bed batch dryers. An indirect forced convection solar dryer for oranges skin was modeled using Hottel Whillier and Bliss model for the solar collector, thermal and mass balances for the dryer chamber [2]. The aim of this work was the determination of the solar collector efficiency, the air temperature outset the collector and the useful power provided by the solar collector to the dryer chamber. Transfer equations were solved using an implicit numerical scheme and Diabolo-Sablier method. The numerical model was validated against experimental results from a blowing with controlled atmosphere. Furthermore, a parametric study which involves two factors, the collector area and the air flow rate, that played a major role in the drying process, leaded to the determination of the collector area for which the functioning of the dryer is optimal. Simat [3] performed an optimization of a mixed mode and indirect mode natural convection solar dryers for maize**.** For the mixed-mode, the drying chamber cover is transparent whereas for the indirect-mode it is opaque. The thermal performance of the collectors for mixed mode and indirect mode solar dryer is described by a set of three equations from energy balance over the cover, absorber and air inside the collector. These equations were solved using an iterative procedure. Simulation models were validated against results from a laboratory solar dryer prototype with experiments carried out under solar simulator. For the same drying capacity, optimization gave a shorter collector area for the mixed mode solar dryer than for the indirect mode dryer. Moreover, the quantity of dry grain obtained from the mixed-mode was less than for the indirect-mode. Bennamoun and Belhamri [4] modeled the performance of a solar batch dryer for agricultural products. This dryer was composed of a flat air collector connected to a heater used in the case of unfavorable climatic conditions. Transfer equations, deduced from thermal and mass balances over the components of the solar collector and the dryer chamber, were solved using Gauss-Seidel iterative method. The coefficient of diffusion was deduced from experimental data and expressed as a function of the temperature and the velocity of the air drying. Variation in the moisture content and the influence of parameters, such as collector area and the drying air temperature were studied. It was shown that the increase of these parameters reduces considerably drying time.

In order to save energy many studies were directed to the design. For example, an indirect solar dryer for

bananas have been simulated to provide design data [5]. The solar collector was placed on the rooftop of the drying building and the dryer chamber inside this building. Transfer equations, deduced from thermal and mass balances over components of the solar collector and the dryer cabined, were solved using the finite difference method. The solar collector area has been optimized using the simulation model combined with an economical model. Janjai et al. (2008) [6] performed a study of a roof-integrated solar dryer for rosella flower and chili. The modeling was carried out for chili and based on transfer equations deduced from thermal and mass balance over various component of the solar dryer. These equations were solved using an implicit numerical scheme and Gauss-Jordan elimination method. In order to validate the mathematical model, an experimental study was performed on the roof-integrated solar dryer. Solar radiation incident on the roof, air temperature in the collectors, air velocity in the collector, relative humidity of ambient air and drying air were measured. A considerable reduction in the drying time as compared the traditional sun drying and a higher quality of dried products in comparison to products quality of traditional drying method were found. Moreover, this dryer system leaded to an added-value and an attractive return on invested capital. A multi tray dryer fitted with an inclined multi pass solar air heater with in-built thermal storage working as a mixed mode was modeled in order to evaluate its performance [7]. The drying chamber was provided with glass windows in three sides (east, south and west) and the north side with an insulating wall. Transfers equations were deduced from thermal and mass balances over the various components of the solar collector and the drying chamber. These equations, linked to the thin layer drying equation used to study the drying rate in the different trays, were solved using a direct numerical method. It will be noted that the solar intensity and ambient temperature are supposed periodic and represented by the Fourier series of six harmonics. Different drying rate has been observed in different drying trays due to the variation in crop temperatures. The drying efficiency increases with increase in weight of the crop.

Concerning the experimental works, Sarsavadia [8] conducted an experimental about a solar-assisted forced convection dryer using electrical energy for the auxiliary heating and running of a blower facilitated with an exhaust air-recirculating duct to study the effect of drying conditions as air temperature, air flow rates and fraction of air recycled on the total energy requirement of drying of onion slices. The total energy requirement and the contribution of the total energy by the solar collector, the blower and auxiliary heating were determined from measures of air flow rates, air and products temperatures, solar irradiance and weight loss of onion slices. It was seen that, at a given air mass flow rate, the contribution to the total energy by the solar collector, the auxiliary heating and blower decreased with increase air drying temperature. At a given air temperature, the contribution to the energy by the solar collector, the blower and the auxiliary heating increased with increase in airflow rate. A solar multi-shelf domestic dryer with a number of useful features as variable inclination to capture more solar radiation, an option to dry products under shade or without shade was performed by Palsingh et al. [9]. The experiments were conducted for drying of fenugreek leaves in the batch modes as well as in the semi-continuous mode. The solar radiation incident on the aperture of the dryer, ambient air temperature, air temperature in the dryer and the weight of the product being dried were recorded. In batch mode, the thermal efficiency reduced during successive drying days while this efficient did not change during all the days of the experiments. The shelf life of the product dried in this domestic dryer has been found to be more than one year.

On the basis of this literature review, it appears that several researchers have proposed numerous models for thin layer drying of various agricultural products (fruits, vegetables, legumes and fish) and for porous media (corn, wheat, cereals, spices) [10-15]. Several types of solar dryer were planned and studied, yielding varying degrees of technical performance. The structure of dryers is depending of the type of product and numerical solutions are often employed to solve these problems because experimental studies

are difficult. Further mathematical models describing heat transfer and mass transfer within the product used the empirical approaches of the drying rate.

It will be noted that the medicinal and aromatic plants have a great importance for both the pharmaceutical industry and the traditional medicine in Maghreb countries [10]. For instance, in Algeria a large number of species vegetal are still dried using the open sun drying. In such conditions, solar-energy dryers appear to be increasingly attractive as commercial propositions [11, 12]. Its low cost and high processing capacity are its main advantages over other techniques. Moreover, according to our knowledge, few studies have been carried out on simulation and optimization of a solar dryer for medicinal and aromatic plants; thus, in this article an experimental and numerical study of an indirect solar dryer for spearmint leaves are performed and the effect of different parameters on the drying are investigated.

The purpose of the present work was to analyze the possibility of using an indirect forced convection solar dryer for spearmint leaves for the typical climatic conditions of Alger (Algeria). Experiments have been conducted on an indirect forced convection solar dryer in order to determine the characteristic drying curve of spearmint leaves (Mentha spicata) used in our drying model. The effective diffusion coefficient and the activation energy of spearmint leaves were also determined.

2. Experimental study

2.1. Experimental set up

The experimental setup, as shown in Fig. 1, consists of an indirect forced convection solar dryer with a flat plate air solar collector, a circulation fan and a cabinet dryer. The solar collector frame is made of aluminum bars; the sides and the bottom are insulated using polyurethane foam of 40 mm thickness. A cooper sheet is allocated behind the transparent cover (clear glass). The cooper sheet and the cover thickness are 4 mm and their area is equal to 2 m^2. This sheet acts as the heat absorber plate painted in black color to maximize the heat absorption from the solar radiation. A gap of 20 mm between the glass and the absorber surface was made. The air to be heated passes between the absorber plate and the insulation. The flat plate air solar collector is placed on a supporting structure at the tilt angle of 36° N (Alger latitude) respect with the horizontal plane. The collector is oriented to south direction to maximize the exposure of solar radiation. One side of the collector is connected to the blower with the help of a PVC tube (80 mm in diameter). The drying chamber was constructed from galvanized iron plate as a parallelepiped enclosure of dimensions 0.93mx0.65m cross sectional area and 1.9m height. The access to the inside of the drying chamber is via an insulated door (0.93 m x 1.9m). There are five trays (L=0.02, W= 0.01 m) for each tray. The tray is made of a wood frame of thickness equal to 0.005 m and a perforated aluminum sheet. Vertical, top and bottom walls as well as the door are insulated using polyurethane foam of thickness equal to 60 mm. The distance from the bottom of the drying chamber to the bottom tray is about 20 cm and a distance of 20 cm among each tray. The bottom side of the drying chamber is a circular tube (15 cm in diameter) connected to a centrifugal fan (220 V, 0.1 kW) and an electrical heater (4 kW, accuracy ± 2%) acting as an auxiliary source. The solar collector is connected to the centrifugal fan with a stainless tube. A thermoregulatory (range 0-100 ° C, 0.1 °C accuracy), connected to a PT100 platinum sensor acting on the auxiliary heating allows the desired air temperature (T_{dry}) at the entrance of the drying chamber. The air flow rate across the solar collector then the drying chamber can be varied between 50 to 600 m^3h^{-1}.

2.2 Experimental procedure

Drying experiments were carried out during July and August 2008 from 8:00 am to 6:00 pm at the Centre of development of Renewable Energy (CDER) of Algiers (Algeria). The spearmint leaves (100.0 g ± 0.001) were uniformly distributed as a single layer on a tray located away the entrance of the dryer. The dryer system is able to dry 20 kg of spearmint leaves. Three drying air temperatures (40, 50 and 60°C) and two

drying air flow rate (0.035 kg.s^{-1} and 0.070 kg.s^{-1}) were selected to examine the influence of temperature and air flow rate on the drying kinetic of spearmint leaves. Before starting the experiments it's necessary to bring the system to steady state conditions. So, an operating period at least of one hour prior to the beginning of each test run is necessary. The dry mass of the spearmint was determined by the dryer oven method (105 °C during 24h). In the experiments, ambient temperature and relative humidity, inlet and outlet air temperature in the solar collector and the drying chamber, the temperatures of the products, the amount of solar radiation and weight loss of spearmint were measured during time first, every 15 min for high moisture content variations then every 20 minutes for weak moisture content variations until the average moisture content reaches a constant value depending on the experimental conditions as the air temperature and air relative humidity.

The measurement of temperatures were performed using thermocouples of type K (0.2 mm diameter) and a Fluke 2625, Hydra data logger with reading accuracy of ± 0.1°C and the solar radiation a Pyranometer (Kipp & Zonen, 0-2000 W m^2, 1mv = 1W m^2) disposed beside the collector. The air mass flow rate is deduced from the air velocity measurements carried out with a thermal anemometer (Hot Wire Anemometer AVM 714) placed in a circular PVC pipe connected to the exit of the drying chamber. The ambient air and recycling air relative humidity were measured with two relative humidity sensors (VAISALA HMP60, Measuring range: 0-100% HR; -40 to +60 °C). Weight loss of spearmint leaves was recording during drying for determination of drying curves by a digital balance in the range of 0-150g with an accuracy of±0.001g.

3. Mathematical modeling

A mathematical model was developed for predicting the performance of this dryer. The assumptions in developing this mathematical model are as follows:

- There is one-dimensional heat-flow across the components of the solar collector and the drying cabinet perpendicular to the air flow direction;
- The ground temperature is equal to the ambient temperature;
- The air is perfectly transparent to the solar radiation and its thermal inertia is negligible;
- There is no shrinkage as drying progress;
- There are no chemical reactions during drying;
- The thermal properties of the product, the air and their moisture content are constants in the range of temperature considered;
- The spearmint leaves on a tray are at the same temperature and have the same moisture content.

3.1. Transfers equations

3.1.1. Equations of solar collector:

Heat transfer inside the solar dryer occurs by convection, radiation and evaporation from the spearmint leaves to the air drying. Further, heat transfer from the cover of the solar collector to the environment takes place by radiation to the sky and by convection due to wind to ambient air. The system is modeled using the time dependent energy balance and mass balance equation [16, 17]. This method is based on the electric analogy relative to a section perpendicular to the air flow rate direction across the collector and the dryer chamber. The solar collector and the dryer chamber are divided respectively into N and M slices perpendicular to the air flow rate direction while considering that the exit of the ith slice is the entrance for the following slice. A node placed in its centre represents every element of the still.

The energy balance for the solar flat plate collector can be divided into 4 regions: glass cover, ...

Based on the above assumptions, the required equations can be written as:

Glass cover

- *External surface*:

$$\frac{m_g \ Cp_g}{\Delta S}\left(\frac{\partial T_{ge}}{\partial t}\right)=\sigma_{sg}+h_{r,ge\text{-}s}\ \left(T_s-T_{ge}\right)+h_{c,ge\text{-}a}\ \left(T_a-T_{ge}\right)+h_{d,ge\text{-}gi}\ \left(T_{gi}-T_{ge}\right)+h_{r,ge\text{-}gr}\ \left(T_{gr}-T_{ge}\right) \quad (1)$$

$$\sigma_{sg}=P_{dir}\ \alpha_{dir,g}+P_{dif}\ \alpha_{dif,g}$$

- Internal surface

$$\frac{m_g \ Cp_g}{\Delta S}\left(\frac{\partial T_{gi}}{\partial t}\right)=h_{r,gi\text{-}p}\ \left(T_p-T_{gi}\right)+h_{c,gi\text{-}p}\ \left(T_p-T_{gi}\right)+h_{d,gi\text{-}ge}\ \left(T_{ge}-T_{gi}\right) \quad (2)$$

Air layer between the cover and the absorber

$$T_{f\_gap}=\frac{T_{gi}+T_p}{2} \quad (3)$$

Absorber

$$\frac{m_p \ . \ Cp_p}{\Delta S}\left(\frac{\partial T_p}{\partial t}\right)=h_{r,p\text{-}gi}\ \left(T_{gi}-T_p\right)+h_{r,p\text{-}insi}\ \left(T_{insi}-T_p\right)+h_{c,p\text{-}f}\ \left(T_f-T_p\right)+\sigma_{sp} \quad (4)$$

With $\sigma_{sp}=\alpha_p\ \frac{P_{dir}\ \tau_{dir}+P_{dif}\ \tau_{dif}}{1-\left(1-\alpha_p\right)\tau_{dir}}$

Air flowing between the insulation and the absorber

$$\dot{m}_f\ Cp_f\ \left(T_f-T_f^*\right)=\Delta S\ h_{c,f\text{-}p}\ \left(T_p-T_f\right)+\Delta S\ h_{c,f\text{-}insi}\ \left(T_{insi}-T_f\right) \quad (5)$$

-Insulation

internal surface:

$$\frac{m_{ins}\ Cp_{ins}}{\Delta S}\left(\frac{\partial T_{insi}}{\partial t}\right)=h_{r,insi\text{-}p}\ \left(T_p-T_{insi}\right)+h_{d,insi\text{-}inse}\ \left(T_{inse}-T_{insi}\right)+h_{c,insi\text{-}f}\ \left(T_f-T_{insi}\right) \quad (6)$$

-external surface

$$\frac{m_{ins}\ Cp_{ins}}{\Delta S}\left(\frac{\partial T_{inse}}{\partial t}\right)=h_{d,inse\text{-}insi}\left(T_{insi}-T_{inse}\right)+h_{r,inse\text{-}gr}\left(T_{gr}-T_{inse}\right)+h_{conv,inse\text{-}a}\left(T_a-T_{inse}\right) \quad (7)$$

3. 2. Cabinet dryer

For the drying chamber, the energy balance is divided into 3 regions: wall, air drying and spearmint leaves.

-Wall

External surface

$$\frac{m_w.Cp_w}{S_{we}}\left(\frac{\partial T_{we}}{\partial t}\right)=h_{d,we\text{-}wi}\ \left(T_{wi}-T_{we}\right)+h_{c,we\text{-}a}\ \left(T_a-T_{we}\right)\ +h_{r,we\text{-}s}\ \left(T_s-T_{we}\right)+h_{r,we\text{-}gr}\ \left(T_{gr}-T_{we}\right) \quad (8)$$

Internal surface

$$\frac{m_w \; Cp_w}{S_{wi}} \left(\frac{\partial T_{wi}}{\partial t}\right) = h_{c,wi\text{-}f} \left(T_f - T_{wi}\right) + h_{d,wi\text{-}we} \left(T_{we} - T_{wi}\right) \quad (9)$$

Drying Air

$$\dot{m}_f \; Cp_f \left(T_f - T_f^*\right) = h_{c,f\text{-}pr} \; S_{pr} \left(T_f - T_{pr}\right) + h_{c,f\text{-}wi} \Delta S_{wi} \left(T_f - T_{wi}\right) + m_{dry} Lv \frac{\partial X}{\partial t} \quad (10)$$

Where $\frac{\partial X}{\partial t}$ is the drying rate expressed in kg water kg^{-1}dm s^{-1}

Spearmint leaves

$$m_{pr} \; Cp_{pr} \left(\frac{\partial T_{pr}}{\partial t}\right) = h_{cv,pr\text{-}f} \; e_{pr} \; \Delta S_{pr} \left(T_f - T_{pr}\right) - m_{dry} Lv \frac{\partial X}{\partial t} \quad (11)$$

Where $Lv = 2.54.10^6 - 2909\, T_{pr}$

$h_{cv,pr\text{-}f}$ is the volumetric heat transfer coefficient ; $h_{cv,pr\text{-}f} = 8.69\; 10^4\; \dot{m}_f^{1.3}$ [6].

The air velocity v_{pr} through the product layer is calculated as follows:

$$v_{pr} = \frac{v_f}{P_O} ; \quad P_o = 1 - \frac{m_{pr}}{\rho_{pr} \; L \; W \; e_{tray}} \quad (12)$$

Where v_f is the air velocity inlet layer of spearmint leaves,
The others heats transfers coefficients are calculated using correlations given in the literature [16, 17]. Three thermal performance parameters are defined: efficiency of the air flat solar collector, drying efficiency and solar fraction. The efficiency of the air flat plate solar collector is defined as the ratio of the total useful energy and the total incident solar radiation energy. The useful energy (Q_u) energy represents the total solar radiation gain of the absorber reduced by heat losses by radiation and convection.

$$\eta_C = Q_U / Q_S \quad \text{With} \quad Q_U = \int_0^{t_{dry}} \dot{m}_f Cp_f \left(T_{f\text{-}out} - T_a\right) dt \;\text{ and }\; Q_S = \int_{t_{ls}}^{t_{cs}} \left(P_{dir} + P_{dif}\right) A_c \, dt \quad (13)$$

The drying efficiency is the thermal energy utilized for the drying divided by the thermal energy available for the drying.

$$\eta_D = \frac{m_v Lv}{Q_u + Q_{aux}} \quad (14)$$

Where m_v is the amount of evaporated water during the drying.

The solar fraction can be defined as the useful energy supplied by the air flat solar collector divided by the thermal energy available for the drying.

$$f = \frac{Q_u}{Q_u + Q_{aux}} \quad ; \quad Q_{aux} = \int_0^{t_{dry}} \dot{m}_f Cp_f \left(T_{dry\_in} - T_M\right) dt$$

Where Q_{aux} is the amount of the energy supplied by the auxiliary source during the drying process and T_M the temperature of the mixing air composed of a fraction T_R of the flow rate of the air outlet the dryer and $(1-T_R)$ of the air flow rate supplied by the solar collector.

(15)

3.3. Numerical methodology

The heat and mass transfer equations were solved using an implicit numerical scheme and the Diabolo-Sablier algorithm. We used an iterative procedure because of the transfer coefficients by convection and radiation depend on temperatures of the various components of the air flat plate solar collector and the drying chamber. For a step time Δt, computation in an element of the solar collector or the drying chamber was declared converged, when the difference between temperatures computed for two successive iterations is inferior to 10^{-3}. Thus, the air temperature is deduced from the knowledge of the useful air power in the element considered. This temperature is supposed equal to the inlet air temperature of the next element. Once the temperatures values have been established in the collector and the drying chamber, the time progressed to t + Δt and computations are carried out until the final moisture content of the product is reached. On the basis of the drying air temperature and relative humidity inside the dryer, the drying parameters (air flow rate, air and product temperature) and the equilibrium moisture content (Xeq) are computed. Using the temperature of the various component of the dryer, the change in moisture content of the entire product for a time interval Δt is calculated from equation (11). Next the equation (10) is resolved. In equations (10) and (11), the drying rate $\partial X/\partial t$ is approximated by an implicit numerical scheme :

$$\partial X/\partial t = (X^{t+\Delta t}(I)-X^{t}(I))/\Delta t$$

The drying rate is computed using the relation (20) deduced from the curve drying characteristics and the equilibrium moisture content, X_{eq} from the relation (19) where R_H is the air drying relative humidity. The knowledge of Xeq and the critical moisture content X_{cri} allow the computation of the drying velocity which is depending on the one hand, the dimensionless moisture content X * (16), the other hand, the initial drying rate (18). The complexity and diversity of the drying mechanisms prevent the use of a single model to characterize the drying process. Thus, experimental studies are necessary to determine the kinetic drying of the product to be dried.

4. Results and discussion

4.1 Experimental results

4.1.1. Characteristic drying curve of Spearmint leaves

The spearmint leaves moisture content evolution during time is shown in Fig. 2. Drying conditions are those of the 16 July 2008 (Fig. 3). The relative humidity of the ambient air varied between 50 and 90%; the ambient temperature between 15 and 31 °C and the global radiation reached the maximum value of 850W m^{-2} at 13:00 (local time). It can be observed that the moisture content decreases quickly because of the interior of the product as well its surface is heated and that weakly bound water from the interior comes to the surface of the spearmint and evaporate from it, characterizing the falling rate. We note for the lowest temperatures that the amount of water evaporates in unit of time gradually decreases, although some quantities of heat are supplied to the spearmint leaves. Our results are in good agreement with these of Doymaz [18] and Kavak Akpinar [19] about the drying of mint leaves.

In the literature there exist numerous studies on drying kinetics and models for various agricultural products. Consequently, various theoretical and empirical equations are used to predict the drying

performance of agricultural products. Among these drying kinetics models, we choose the curve drying characteristics (CDC).The CDC [20] consists in normalizing the kinetics of the drying in a theoretical model from experimentations. The use of the Van Meel [21] concept of CDC allows representing the drying rate period of the spearmint leaves obtained for different drying conditions by a single normalized drying curve. The drying rate is normalized as:

In abscissa: $$X^* = \frac{X(t) - X_{eq}}{X_{cri} - X_{eq}} \quad (16)$$

In ordinate**:** $$f^* = f(X^*) = \left(-\frac{dX}{dt}\right)_t / \left(-\frac{dX}{dt}\right)_I \quad (17)$$

X_{cri} : critical moisture content defined as the average moisture content where the constant rate period ends and the falling rate period starts. $\left(-\frac{dX}{dt}\right)_I$: drying velocity during the first drying phase.

It was noted that the drying kinetics of the spearmint leaves reveals no constant period (Fig. 3). In order to apply the Van Meel concept of (CDC) for this product, we replace as it was done in various studies about biological products X_{cri} by X_0 and $\left(-\frac{dX}{dt}\right)_I$ by $\left(-\frac{dX}{dt}\right)_0$

The initial drying rate $(dX/dt)_0$, is deduced from Fornell [22,23]:

$$\left(-\frac{dX}{dt}\right)_0 = a\, v_{pr}^b (T_f - T_{wb}) \quad (18)$$

Where T_{wb} is the wet-bulb temperature. a and b are determined from measures of the moisture content and using the square method: a = 7.25 10^{-4} and b = 2.57. The equilibrium moisture content, X_{eq} is computed from the following relation [22, 23]:

$$X_{eq} = 1.161 + 106.936 R_H - 311.778 R_H^2 + 264.997 R_H^3 \quad (19)$$

The evolution of the moisture content X (t) was deduced from the product weight loss during the drying process. Measures were performed every 15 minutes at the beginning of the drying process where the moisture variation is great than then every 20 minutes for weak moisture content variations until the average moisture content reaches a constant value depending on the experimental conditions as the air temperature and air relative humidity. The average constant value was about X_f =0.47(kg of water / kg of dry product).
A set of 6 experiments were conducted to develop a drying model to simulate the drying curves of spearmint leaves. The study for three air drying temperature 40, 50 and 60 °C and two air flow rate equal to 0.035 and 0.07 kg.s^{-1} of the evolution of the normalized drying rate f* as a function of reduced moisture content, X*, leads to a grouping of different values around a single mean curve : the CDC (Fig. 4). The equation of the CDC was determined using the least squares method. The criterion used to evaluate the fit accuracy was a residual standard error (S_R=0.0506) and a multiple R squared (R^2 = 0.9515). The highest value of R^2 and lowest value of S_R indicated the goodness of the fit of the experimental data.

$$f^* = \left(\frac{(-dX/dt)}{(-dX/dt)_0}\right) = 2{,}17683X^* - 8.02535X^{*2} + 20.94598X^{*3} - 25.6662X^{*4} + 11.68 \quad (20)$$

4.1.2 Effective diffusion coefficient

The diffusion coefficient for each drying condition was determined from experimental data using the following widely used equation [18, 19]:

$$\mathrm{Ln}(X^{*})=\mathrm{Ln}\left(\frac{8}{\pi^{2}}\right)-\left(\frac{\pi^{2}D_{eff}\,t}{4e_{sp}^{2}}\right) \quad (21)$$

Where (D_{eff}) represents the effective diffusion coefficient and (e_{sp}) the half thickness of a spearmint leave.

Fig. 5 shows a plot of ln (X*) versus the time for three air drying temperature (40°C, 50°C and 60°C) and an air mass flow rate equal to 0.03 kg.s^{-1}. It can be seen that the slope of the curve, i.e. diffusivity decreases as the drying time increases. This is expected as the shrinkage and hardening of the material offer increasing resistance to moisture diffusion. Diffusion coefficients of spearmint leaves for these three air drying temperature are presented in Table 1. These values are comparable to some others data reported in the literature [18] about mint leaves. We note that the diffusion coefficient increases as air temperature increases.

4.1.3 Activation energy

The effective diffusivity coefficient can be related to air temperature by Arrhenius expression [18, 19, and 24] as:

$$D_{eff}=D_{0}\exp\left(-\frac{Ea}{R(T_{f}+273.15)}\right) \quad (22)$$

Where, D_0 constant (23.49 10^{-3} m^2 s^{-1}), Ea: activation energy (kJ.mol^{-1}), T: air temperature (°C) and R: universal gas constant (kJ mol^{-1} K^{-1}). Eq. (24) can be rearranged in the form of:

$$\mathrm{Ln}\left(D_{eff}\right)=\mathrm{Ln}\left(D_{0}\right)-\frac{Ea}{R\,(T_{f}+273.15)} \quad (23)$$

The plot of $\mathrm{Ln}(D_{eff})$ versus $1/T_f$ leads to the activation energy (Fig. 6). From this figure, E_0 is equal to 54.30kJ mol^{-1}. This value is an agreement with the activation energy one of various herbs. In this way, Doymaz, [18] found for mint leaves a value equal to 62.96 kJ mol^{-1}.

4.2 Numerical results

Simulations were carried out for meteorological data of Algiers (Algeria) based on the notion of a typical day (Fig. 7), a weight of spearmint leaves varying between 5 and 20 kg; an air mass flow rate in the range of 0.14 to 0.30 kg s^{-1}; five air-drying temperatures 30, 35, 40, 45, and 50°C. The initial and final moisture content of the product are respectively equal to X_0=5 and X_{final} =0.47 (kg water.kg^{-1} dry matter). We investigate also the effects of air recycling rate using three values 25%, 50% and 75%. We consider the drying cycle as the time between sunrise and sunset of the typical day.

4.2.1. Drying curve

Simulations were carried out to investigate the effects of various drying parameters such as air mass flow rate, air drying temperature and weight of fresh product on drying time. We performed theses simulations for determining the functioning parameters for which the drying time is inferior to the period of sunshine. In order to analyze the effect of the weight of spearmint on the drying duration, the computations were performed for four thicknesses of spearmint leaves 5, 10, 15 and 20 cm corresponding respectively to a mass of 5, 10, 15 and 20 kg of product. Figs. 8, 9 and 10 show the effect of the air mass flow rate, the weight of spearmint leaves and the air drying temperature on the drying duration for three air recycling rate (25, 50 and 75%). We note that the drying time decreases as the air mass flow rate increases whatever the layer thickness of spearmint leaves and the air-drying temperature values used in this study. In fact, the convective

heat and mass transfers between the spearmint leaves and the drying air are all the more high that the air velocity is important. The drying time was reduced significantly as the air drying temperature increases because the pressure vapor of the surface spearmint leaves is related to its temperature. Consequently, an increase of the air drying temperature leads to an augmentation of the surface pressure vapor; so the air around the products for which the pressure vapor is inferior to the product surface one, can pick up the moisture from the spearmint leaves. We note that these results are in agreement with experimental results presented above (Fig. 2). The increase of the air recycling rate leads to a decrease of the drying duration notably for low weight of spearmint leaves. Therefore, several scenarios are eliminated; so that the acceptable drying duration is less than that of the period of sunshine. From Figs. 8, 9 and 10, we note that for all values of the weight of the spearmint leaves, the low air flow rate values, the drying duration is inferior to the sunshine one for air temperatures drying used in our simulations.

4.2.2 Collector and dryer efficiency

In general the air mass flow rate and the area collector are the most important parameters affecting the performance of the solar collectors. So, the influence of the air mass flow rate and the area collector on the air outlet temperature and the efficiency was studied. Fig .11 shows that the collector efficiency is the more important that the area collector is small. For this area collector the efficiency increases as the air mass flow rate increases. We note that for an area collector superior to 6 m^2, the collector efficiency remains constant as the air mass flow rate increases.

Results presented above show that important weight of spearmint leaves increase the amount of heat for the drying process, small air drying temperature decrease the heat quantity supplied by the auxiliary source and high air mass flow rate yield high drying efficiency. Fig. 12 shows the drying efficiency during a year for different air mass flow rate. The drying efficiency displays a maximum value during summer days because of the atmospheric conditions of Algiers region contributes to an increase of the evapo-transpiration of vegetations and of the evaporation of water during these days. The augmentation of air mass flow rate leads to an increase of the drying efficiency. A higher air mass flow rate will speed up the evaporation process, while a lower air mass flow rate will slow down the process because heat and mass transfer coefficients between spearmint leaves and air are depending on air velocity.

4.2.3. Solar fraction

The solar fraction is lower in winter (Fig. 13). In fact, the solar fraction depends on solar duration: the days of July and August represent the greatest day length (15 hours) and the daily global radiation is about 7.5 kWh m^{-2} per day. We note that the solar fraction reaches higher values for low air flow rate. Consequently, it is necessary to proceed to a choice of the solar fraction value to deduce the air flow rate for which the efficiency dryer is maximal.

We plot the evolution of the solar fraction versus the area collector for these drying conditions (Fig. 14). The analyze of this figure shows that on the one hand, the solar fraction increases as the area collector increases because the amount of useful heat provided by the air solar collector is depending essentially of the collector area and the drying conditions on the other hand, the increase of the weight of spearmint leaves leads to a decrease of the solar fraction because the heat quantity supplied to the product for its drying is all the more as the mass of spearmint leaves is important. However, we note the existence of an area value from which the solar fraction increases slowly as the solar collector area increases; this demonstrate that it's not necessary to use a higher collector area to increase the solar fraction. Fig.15 depicts the effect of the air recycling rate and the air flow rate on the solar fraction. We note that the solar fraction increases with the air flow rate until a maximum value depending of the air recycling rate, then decreases as the air flow rate increases. The solar fraction is all the more great than the air recycling is important.

We plotted in Figs.16 and 17 the maximum value of the solar fraction (Fig.14) versus the drying air temperature and the weight of the spearmint leaves. The maximum solar fraction decreases as the weight of the spearmint leaves increases because of the amount of heat quantity required for the drying process is depending of the moisture quantity to remove from the product and consequently of the weight of spearmint leaves. As it has been reported previously the solar fraction decreases as the air flow rate increases because of the air temperature outlet the solar collector which decreases with the increases of the air flow rate.

Consequently, the amount of heat supplied to the dryer by the auxiliary source increases with the drying air temperature. From these figures we can deduced that the maximum solar fraction can be obtained with low weight of spearmint leaves, high air recycling rate and for drying air temperature about 30°C.

5. Conclusion

An experiment and modeling study of an indirect forced convection solar dryer have been developed for spearmint leaves. On the basis of discussions in various sections, the following conclusions can be inferred:

-The solar fraction reaches its maximum values for small values of air mass flow rate;

-The required drying time increases as the spearmint weight increases or drying air temperature and air flow rate decrease;

-The diffusivity decreases as the drying time increases

-The activation energy is close to the one of various herbs,

-The area collector has a considerable effect on the solar fraction; therefore, for a fresh product weigh of 10 kg and a collector area of 2 m^2, the solar fraction and the efficiency of the solar collector are about 60% and 50% respectively.

References

[1] Pratoto A, Daguenet M, Zeghmati B. A simplified technique for sizing solar-assisted fixed-bed batch dryers: application to granulated natural rubber. Energy Convers Manage 1998; 39(9): 963-971.

[2] Belghit A, Belahmidi M, Bennis A, Boutaleb B.C., Benet S. Etude numérique d'un séchoir solaire fonctionnant en convection forcée. Revue Générale de Thermique 1997; 36: 837-850.

[3] Simate N. Optimization of mixed-mode and indirect-mode natural convection solar dryers. Renew Energy 2003; 28: 435–453.

[4] Bennamoun L, Belhamri A. Design and simulation of a solar dryer for agriculture products. J Food Eng 2003; 59:259-266

[5] Smitabhindu R, Janjai S, Chankong V. Optimization of a solar-assisted drying system for drying bananas. Renew Energy 2008; 33: 1523–1531.

[6] Janjai S, Srisittipokakun N, Bala B.K. Experimental and modelling performances of a roof-integrated solar drying system for drying herbs and spices. Energy 2008; 33(1): 91-103.

[7] Jain D. Modeling the system performance of multi-tray crop drying using an inclined multi-pass solar air heater with in-built thermal storage. J Food Eng 2005; 71: 44–54.

[8] Sarsavadia PN. Development of a solar-assisted dryer and evaluation of energy requirement for the drying of onion. Renew Energy 2007; 32: 2529–2547.

[9] Palsingh P, Singh S, Dhaliwal S. Multi-shelf domestic solar dryer. Energy Convers Manage 2006; 47: 1799-1815.

[10] Cheriti A, Rouissat A, Sekkoum K, Balansard G. Plantes de la pharmacopée traditionnelle dans la région d'El Bayadh (Algérie). Fitoterapia 1995; 66(6): 525-538.

[11] Rajkumar P, Kulanthaisami S. Vacuum assisted solar drying of tomatoes slices. ASABE Annual International Meeting. Portland Oregon; 9-12 Jul.2006.

[12] Ekechukwu O.V, Norton B. Review of solar energy system II: An overview of solar drying technology Energy. Energy Convers Manage 1999; 40 (6): 615-655.

[13] Panchariya P.C, Popovic D, Sharma A.L. Thin-layer modelling of black tea drying process. J Food Eng 2002; 52: 349–357.

[14] Ratti C, Mujumdar AS. A mathematical model for solar batch drying of carrots. Solar Energy 1997; 60 (3–4):151–157.

[15] Steinfeld SI. Simulation model for solar thin layer drying process. Drying Technology 1986; 4: 535-542.

[16] Duffie J.A, Beckman W. A. Solar engineering of thermal process. New York : John Willey & sons; 1991.

[17] Daguenet M. Les séchoirs solaires : Théorie et Pratique. U.N.E.S.C.O. 1985

[18] Doymaz I. Thin-layer drying behavior of mint leaves. J Food Eng 2006; 74: 370–375.

[19] Kavak Akpinar E. Drying of mint leaves in a solar dryer and under open sun: Modeling performance analysis. Energy Convers Manage 2010; (51): 2407-2418.

[20] Lahsasni S, Kouhila M, Mahrouz M. Adsorption–desorption isotherms and heat of sorption of prickly pear fruit (Opuntia ficus indica). Energy Convers Manage 2004; 45: 249–61.

[21] Van Meel DA. Adiabatic convection batch drying with recirculating air. Chem Eng Science 1958; 9: 36–44.

[22] Belghit A, Kouhila M, Boutaleb B.C. Approche Expérimentale de la Cinétique de Séchage de la Verveine (Lippia Citriodora). Rev Energ Ren 1999; 2: 87-97.

[23] Kouhila M, Belghit A, Kaoua M, Daguenet M. Etude expérimentale du séchage convectif de la menthe dans un séchoir modulaire polyvalent à chauffage partiellement solaire. Revue Energie Renouvelable. Physique Energétique 1998: 1– 5.

[24] Doymaz I, Pala M. Hot-air drying characteristics of red pepper. J Food Eng 2002; 55:331–335.

Figures

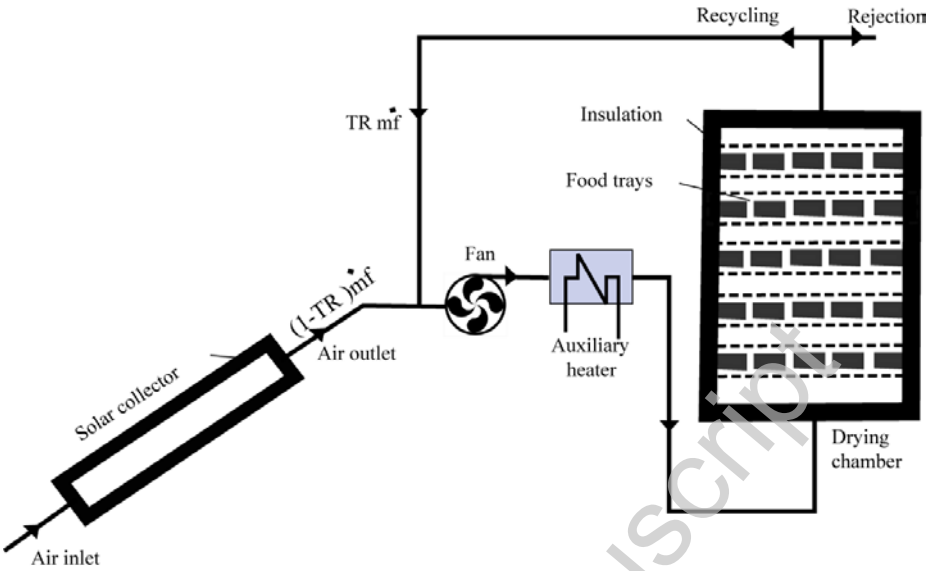

Figure 1: Schematic representation of the drying system

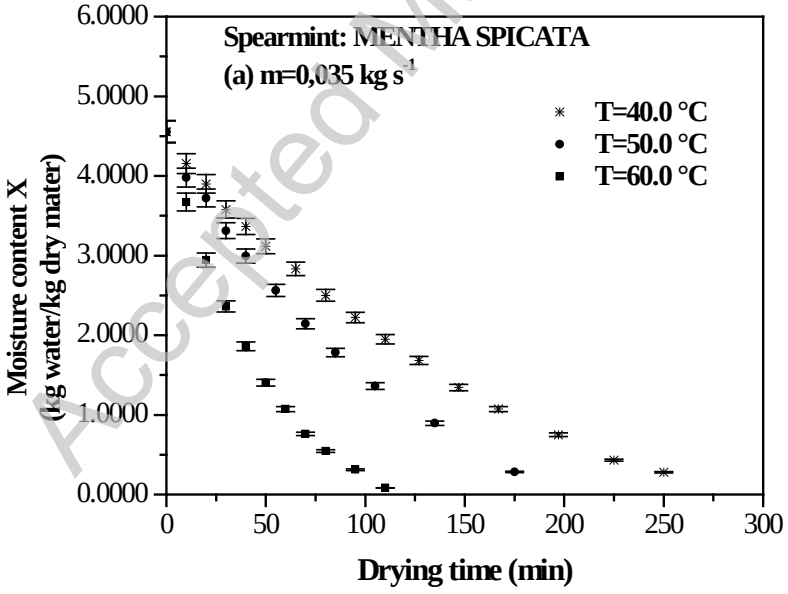

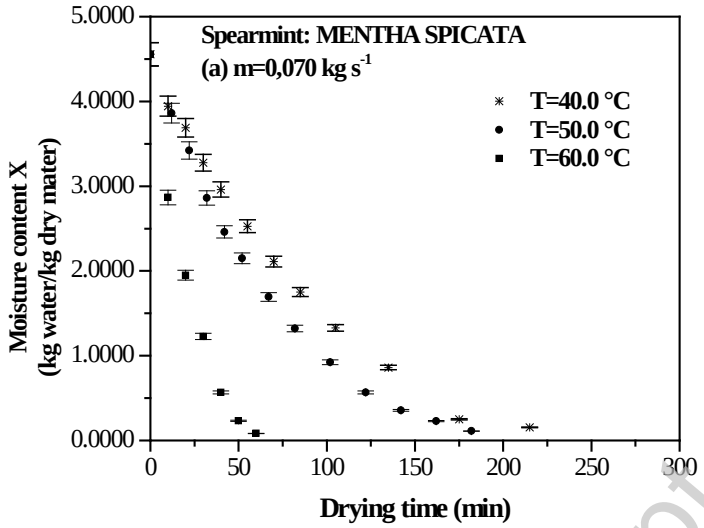

Figure 2: Evolution of moisture content versus time. Effect of air-drying temperature

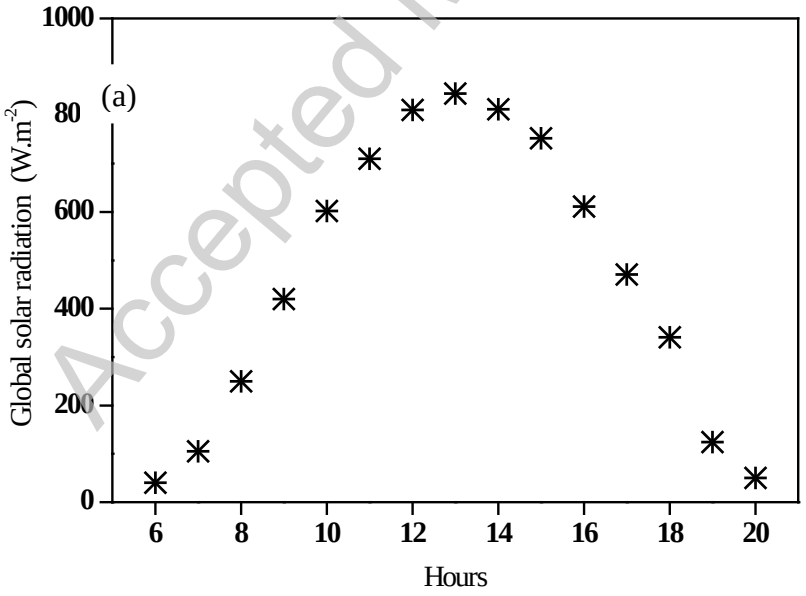

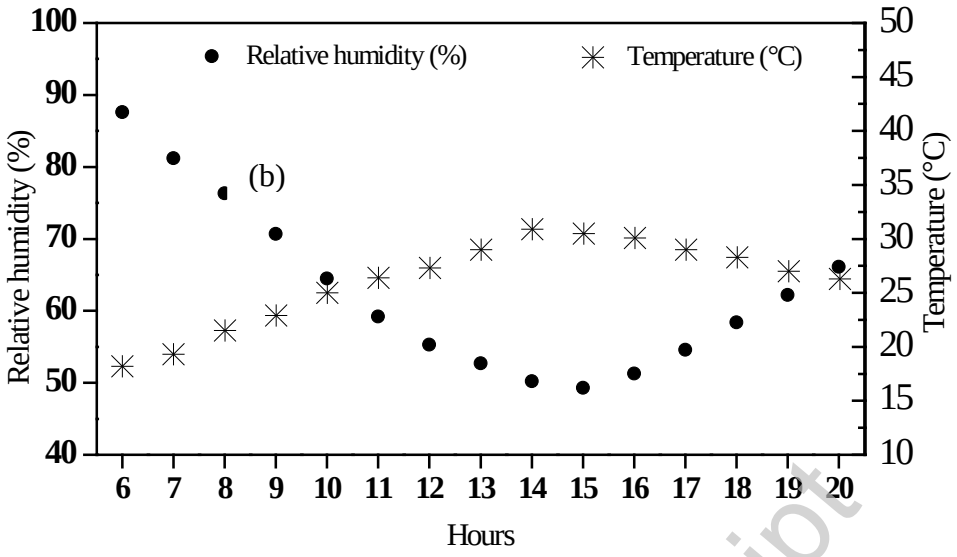

Figure 3: Meteorological data in Algiers (Algeria). (a) :Global solar radiation

(b): Relative humidity and temperature

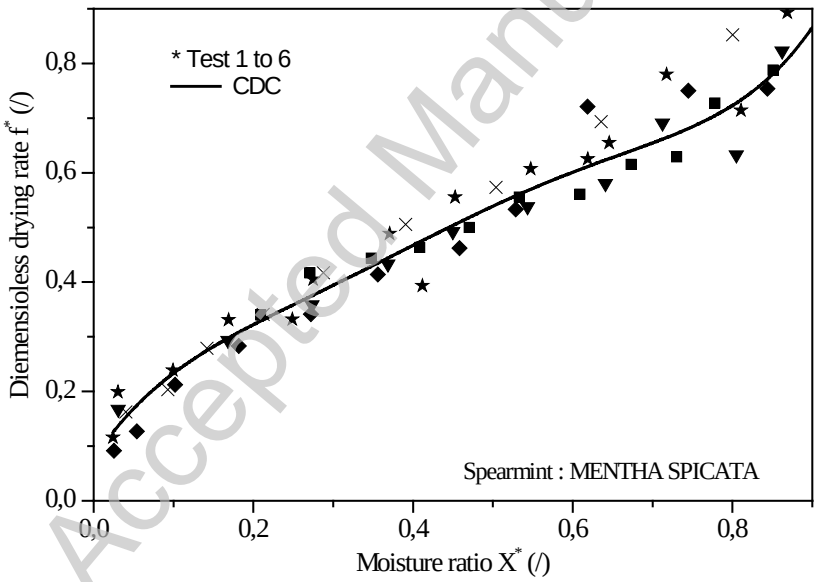

Figure 4: Characteristic drying curve (CDC) of Spearmint leaves

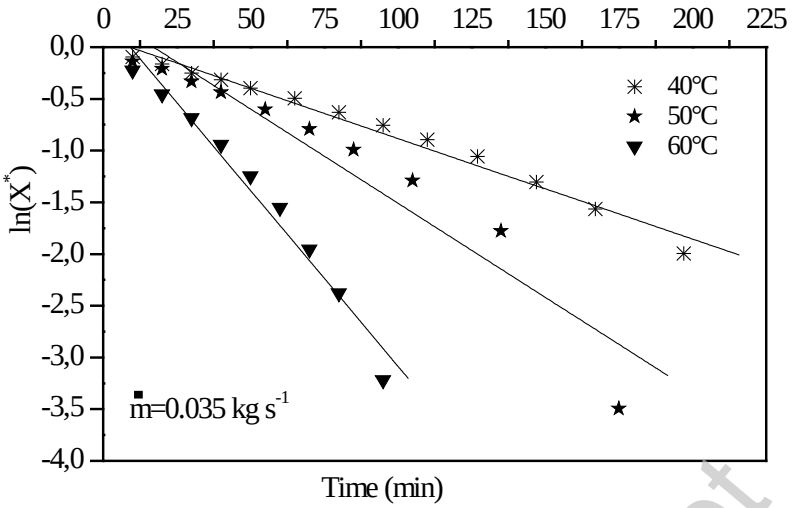

Figure 5: $Ln(X^*)$ versus time

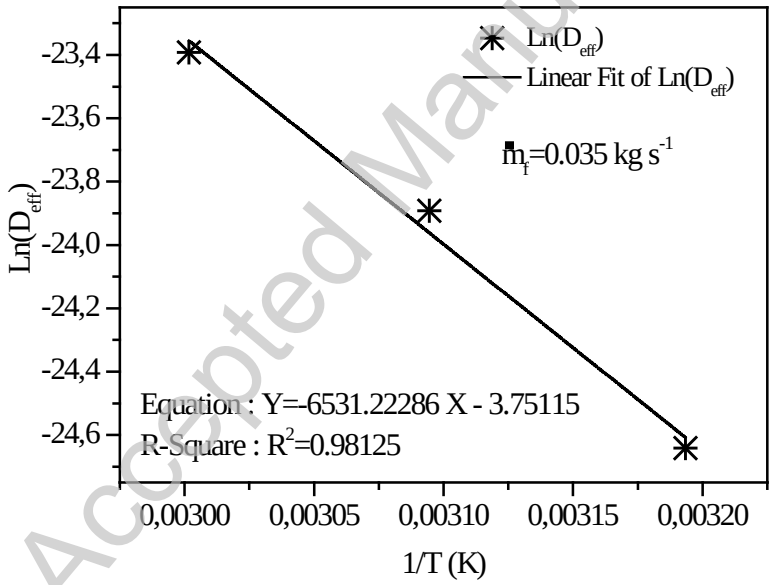

Figure 6: Effective diffusivity versus air temperature

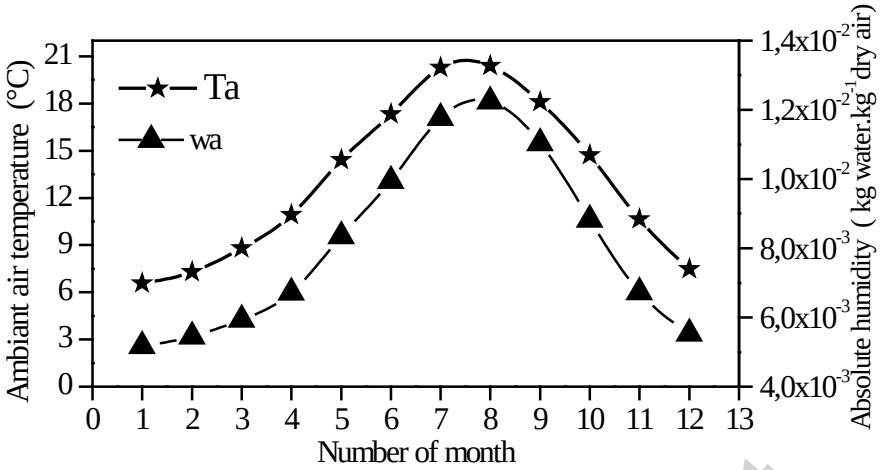

Figure 7: Monthly Average diurnal variations of ambient temperature and absolute humidity in Algiers

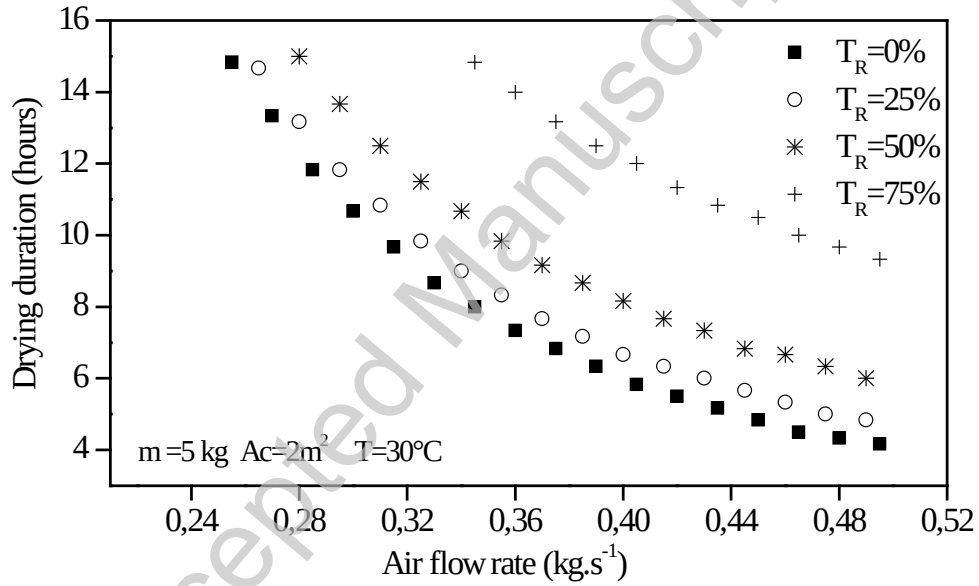

Figure 8: Evolution of the drying duration versus the air mass flow rate

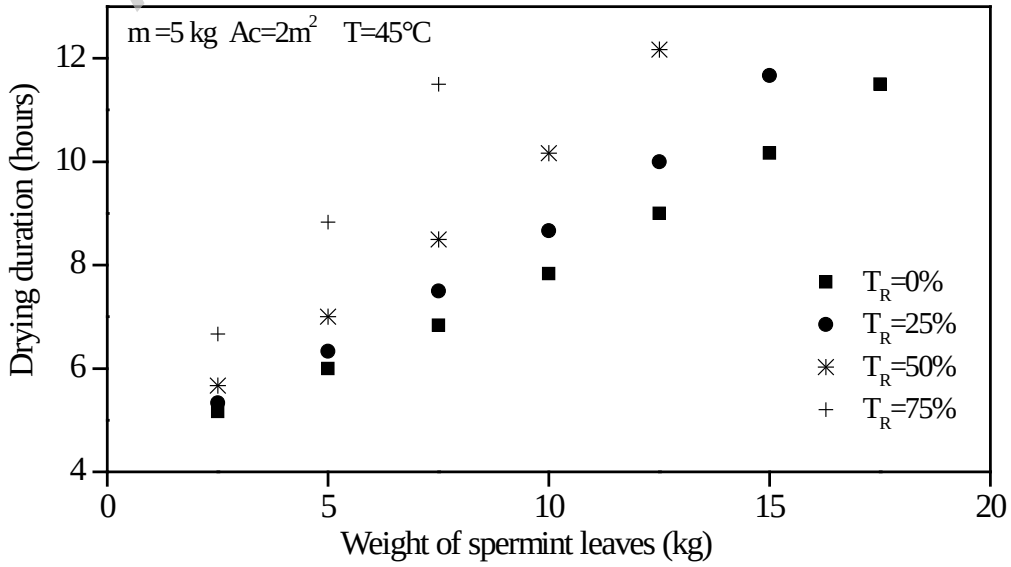

Figure 9: Evolution of the drying duration versus the weight of spearmint leaves

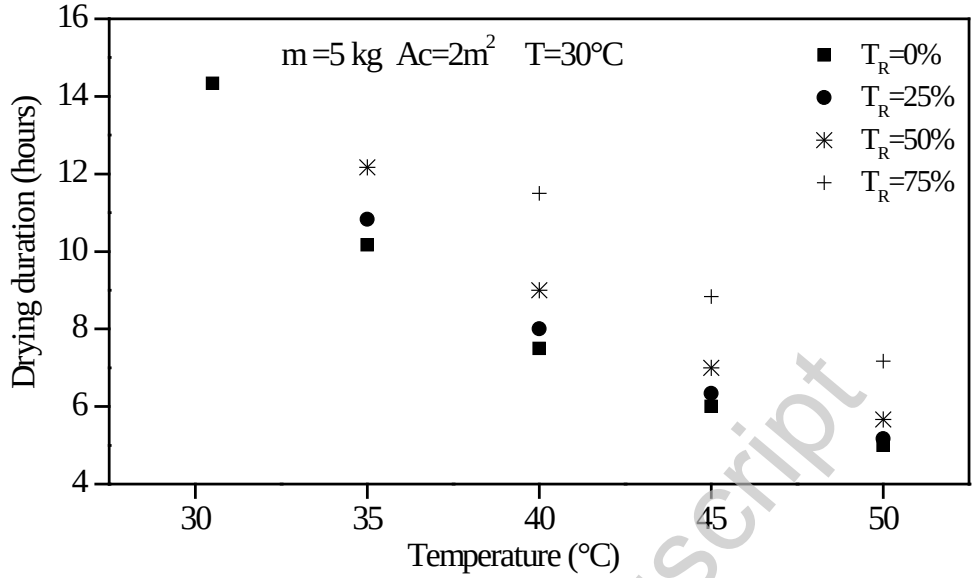

Figure 10: Evolution of the drying duration versus the air drying temperature

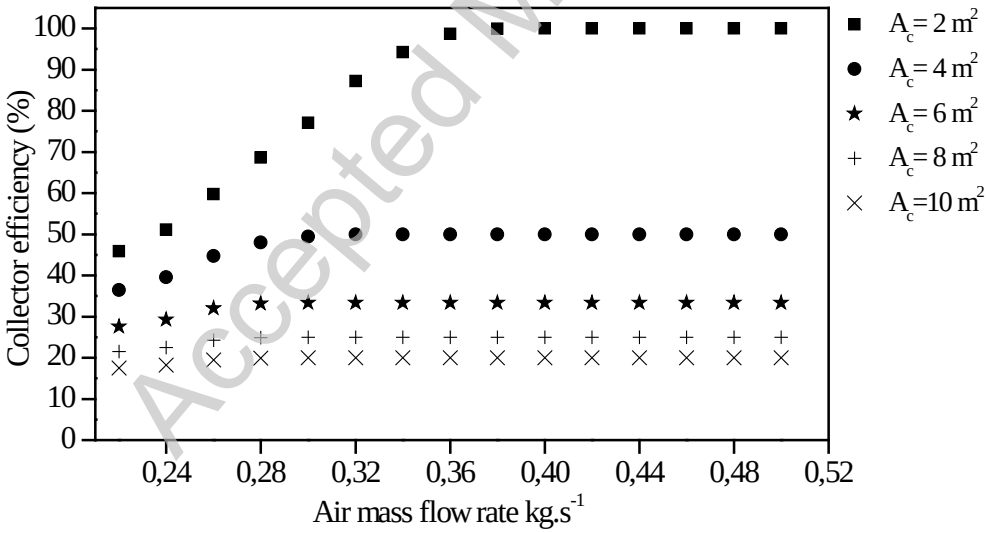

Figure 11: Evolution of the solar collector efficiency versus the air mass flow rate: Effect of the area collector

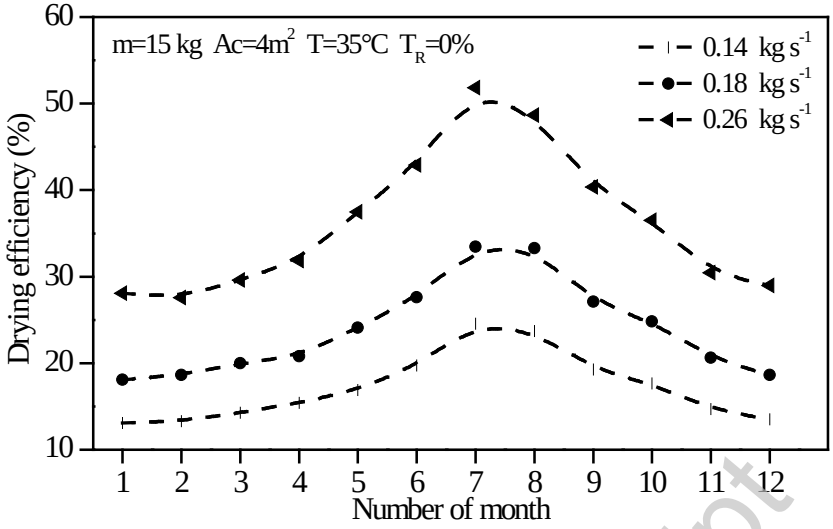

Figure 12: Evolution of the evaporation efficiency during a year: Effect of air mass flow rate

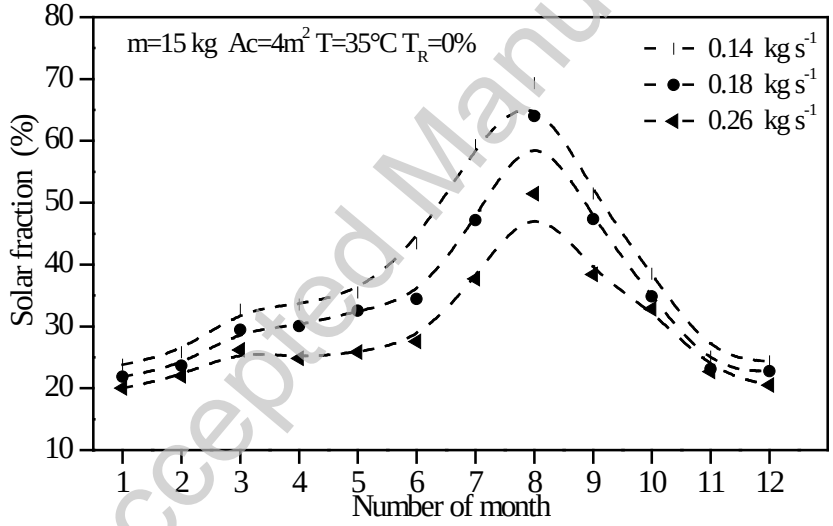

Figure 13: Evolution of the solar fraction during a year: Eeffect of air mass flow rates

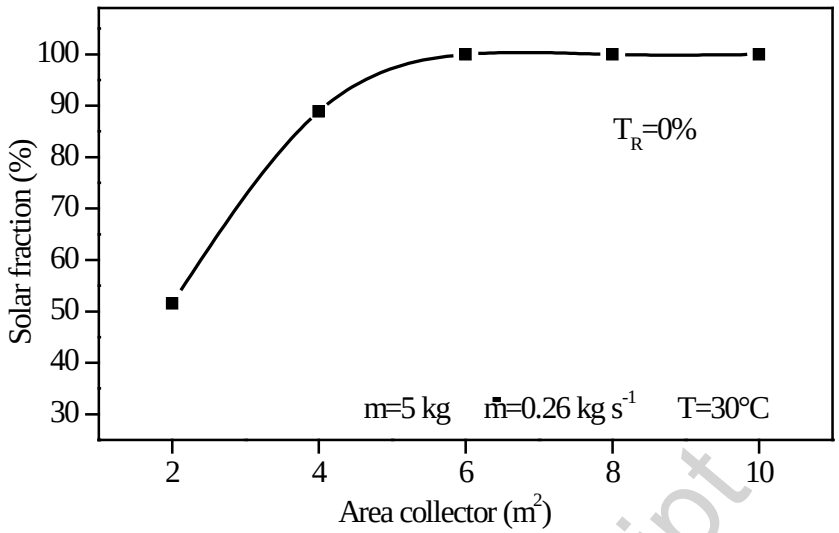

Figure 14: Evolution of solar fraction versus the area solar collector

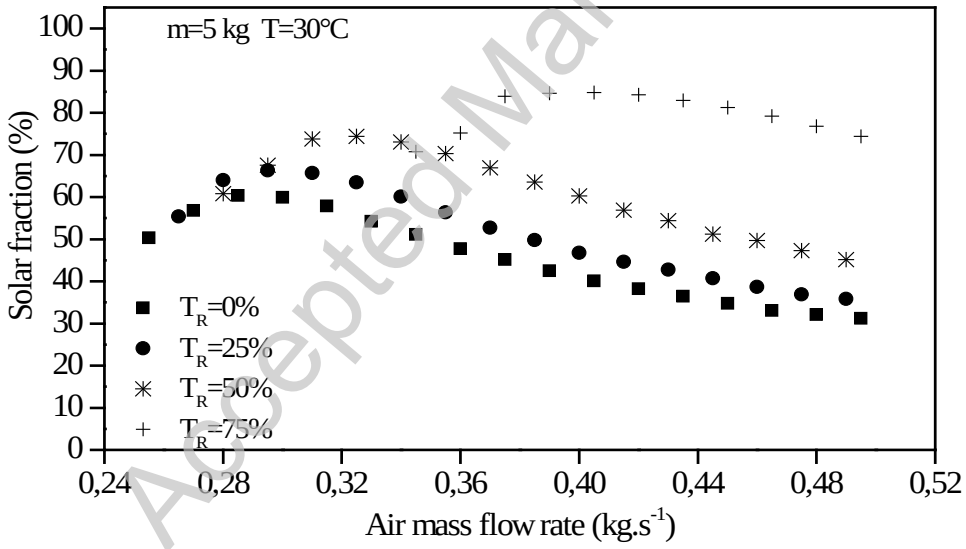

Figure 15: Evolution of solar fraction versus the air mass flow rate

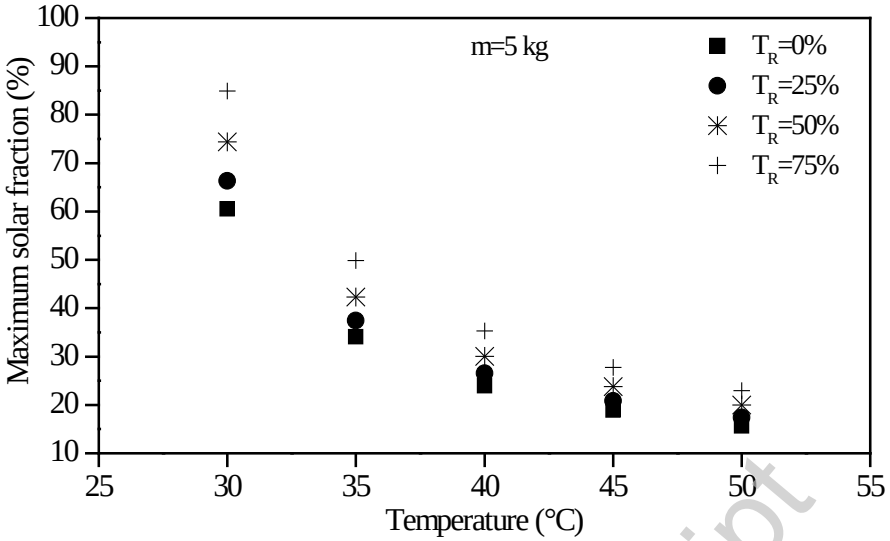

Figure 16: Evolution of the maximum solar fraction versus the air drying temperature

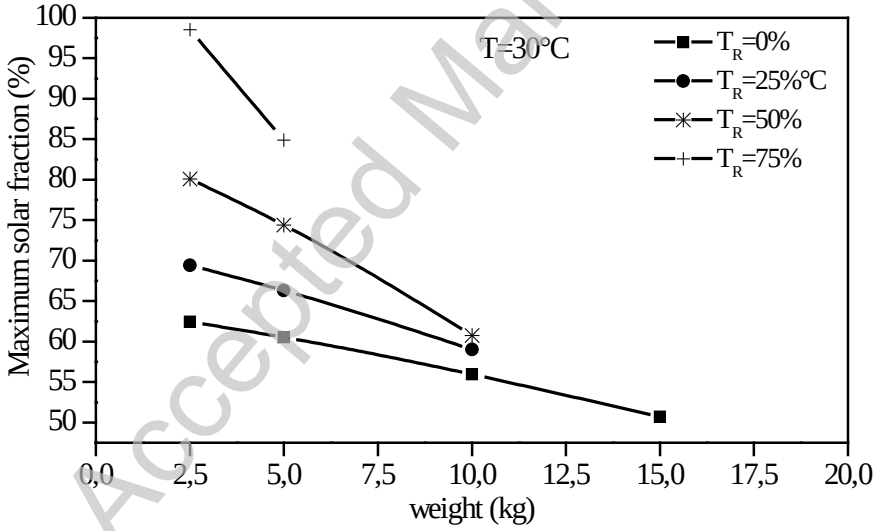

Figure 17: Evolution of the maximum solar fraction versus the weight of spearmint leaves

Table

Table 1: Diffusion coefficients of spearmint leave drying at different drying conditions

Temperature (°C)	Diffusion coefficient, (D_{eff}) m^2/s
40	$1.9871\ 10^{-11}$
50	$4.2059\ 10^{-11}$
60	$6.935\ 10^{-11}$